Improving the ft value of ^{37}K via a precision measurement of the branching ratios

A. Ozmetin

(Dated: April 18, 2020)

I. INTRODUCTION

As part of the TRIUMF Neutral Atom Trap (TRINAT) collaboration, our goal is to search for physics beyond the standard model via precision measurements of the polarized angular correlations of the isobaric analogue β^+ decay of ^{37}K (see Fig. 1). A recent measurement of the β asymmetry parameter, A_β, has reached 0.3% precision [1] which, when combined with the comparative half-life or ft value, was used to improve the value of V_{ud} for this decay as well as search for right-handed currents. Plans are underway to improve the A_β measurement, at which point uncertainties in the ft value will no longer be negligible. Presently, the uncertainty in the ft value is dominated by the 97.99(14)% branch to the ground state following an improved half-life measurement performed at the Cyclotron Institute [2].

The 1997 measurement which dominates the present value of the branching ratio [3] was limited by the absolute efficiency of the HPGe detector. Using the fast-tape-transport system at the Cyclotron Institute and the world's most precisely calibrated HPGe, we measured the decay of ^{37}K to significantly improve the branching ratio and hence the ft value.

II. THE BRANCHING RATIO EXPERIMENT

A. Producing and Collecting ^{37}K at the Cyclotron Institute

The ^{37}K was produced via the $p(^{38}\mathrm{Ar}, 2n)^{37}$K reaction in inverse kinematics at a beam energy of 29 MeV$/u$ from the K500 cyclotron. Using the Momentum Achromatic Recoil Spectrometer (MARS), the ion beam was purified to over 99.7% before passing through the heavy ion (HI) scintillator and a stack of Aluminium degraders optimized so as to stop the ^{37}K in the centre of the aluminized-Mylar tape. The activity was then quickly transported between a plastic scintillator and a high-purity Germanium (HPGe) detector to observe β-γ coincidences using the fast-tape transport system depicted in Fig. 2.

Our measurement cycle begins by depositing the ^{37}K in the tape for $t_{\mathrm{collect}} = 2.5$ s before

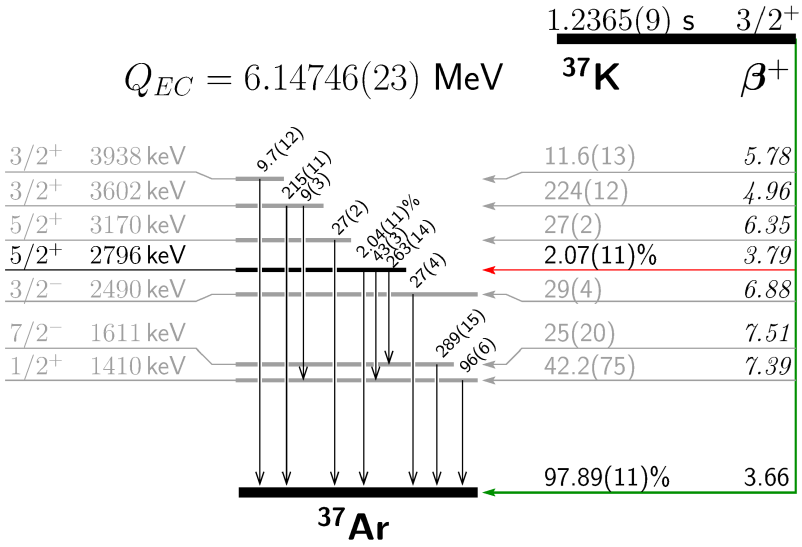

FIG. 1. The β^+ decay of ^{37}K. Unless otherwise noted, the β and γ branching fractions are quoted in parts-per-million. The transition of interest, highlighted in green, is the $J^\pi = 3/2^+ \rightarrow 3/2^+$ decay to the isobaric-analogue ground state in ^{37}Ar.

being moved to the measurement position in $t_{\text{move}} \sim 160$ ms. The data acquisition system is then enabled to collect the γ and β data for $t_{\text{count}} = 2.5$ s

B. Data Acquisition

The HPGe detector is used to identify the energy and measure the total number of γ rays produced in the decay. In order to deduce the branching ratio, it is critical to have a precise understanding of the detector's efficiency response as a function of energy. The absolute efficiency of this detector has been characterized using multiple sources and Monte Carlo simulations, and is presently the most-precisely calibrated HPGe in the world with a fractional uncertainty of $\pm 0.2\%$ over the energy range $50 \leq E_\gamma \leq 1400$ keV [4], and $\pm 0.4\%$ from $1.4 - 3.5$ MeV [5]. The thin 1-mm BC404 plastic scintillator provides a β coincidence with the γ, and is placed opposite the HPGe to minimize β bremmstrahlung summing with the γ rays.

When there is a hardware coincidence between the HPGe and scintillator, the data acquisition system records all of the information collected by the system [6]: the time since the last tape movement, t_{cycle}; the relative timing of the β and γ, t_β and t_γ respectively; the energy signal

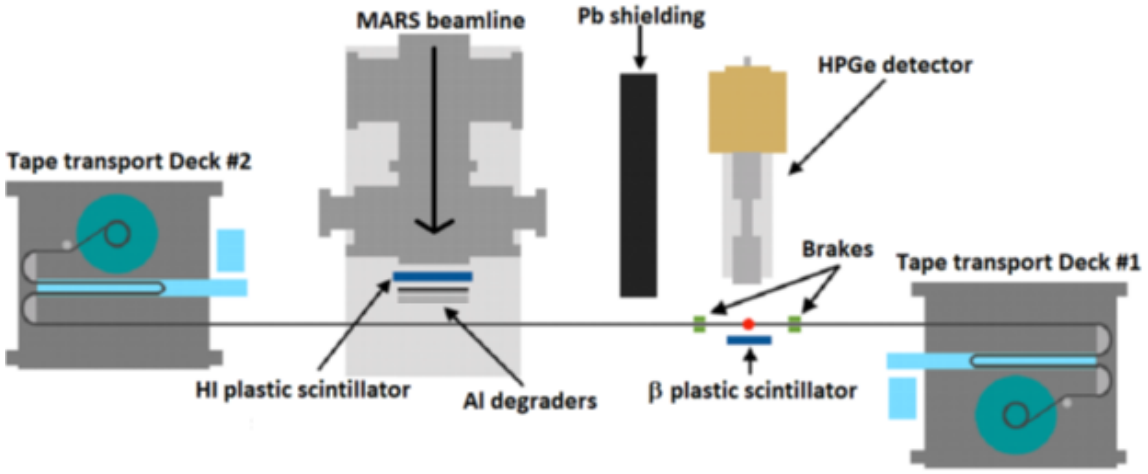

FIG. 2. Outline of the experimental set-up to observe β-γ coincidences. The ^{37}K beam exits the MARS beamline and is transported to the detection area using the fast-tape-transport system.

from the HPGe, E_γ; and the energy signal from the plastic scintillator, ΔE_β. The scintillator ΔE_β signal is stored in singles by a multi-channel scalar, providing a summed β spectrum, however only β-γ coincident events save the complete information event-by-event. Similarly, the γ singles detected over each cycle are scaled and stored in the event file; these are needed to account for dead-time losses in the HPGe [6].

III. DATA SELECTION

A. Filtration of bad cycles

Although reliable, the tape-transport system is not flawless and occasionally does not stop in the ideal position, perfectly between the HPGe and scintillator detectors. These deviations from the center threaten the validity of the obtained efficiencies which were determined for activities placed along the detection axis. In order to not pollute the data pool with unaccounted systematics, cycles that did not stop in the correct position must be removed. Fortunately this phenomenon can be easily identified by looking at the β-to-HI ratio. The HI scintillator counts all ions coming out of MARS with $\approx 100\%$ efficiency, and this rate is roughly constant over an entire run. The rate of βs, however, depends sensitively on the position of the tape cycle-by-cycle, and so if the β/HI ratio is low for a given cycle, that is a clear indication the

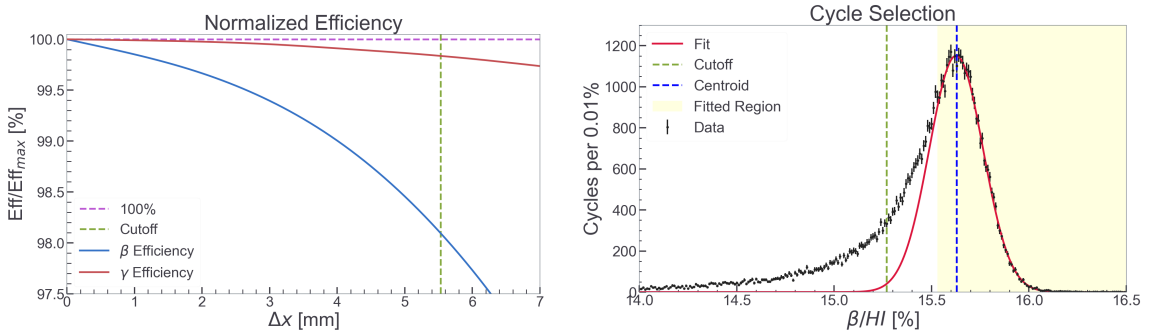

(a) Relative efficiency of the scintillator and HPGe versus the displacement of the position of the activity. Here zero displacement corresponds to the activity being placed on the axis defined by the centres of the two detectors.

(b) The number of cycles versus the ratio of βs to heavy ions. The cutoff for the minimum β/HI defining *good* cycles is based on the allowable deviation in the γ efficiency given our precision goal of $< 0.1\%$ in the branching ratio.

FIG. 3. Plots used to determine which cycles to remove due to improper placement of the activity after the tape transport.

activity was not moved to the proper location and it can be removed from the data pool.

In Fig. 3b, all the cycles are binned based on their β/HI ratios, then fitted to a Gaussian using only the right side of the peak since this is the part that corresponds to the random distribution rather than being influenced by incorrect tape movement. A Monte Carlo simulation was written to calculate the geometric effect of a misplacement on the relative efficiencies of both detectors. Although the β detector efficiency does not have a direct influence on the branching ratio, the efficiency of the γ detector greatly affects the results.

In order to ensure the final branching ratio was not dominated by systematics from the γ efficiency, we require the deviation to be $\Delta\left(\epsilon_\gamma/\epsilon_\gamma^{\max}\right) < 0.2\%$. In this way, the uncertainty contribution of tape deviation is kept way below $< 0.1\%$. As seen in Fig. 3a, this corresponds to a maximum tape mispositioning of 5.5 mm and a maximum β efficiency deviation of 1.9%. Therefore, when filtering runs based on their β/HI ratio, we required this fraction to be $> 98.1\%$ of the central value, *i.e.* a cutoff of β/HI > 15.3; cycles with a ratio below this cutoff were discarded (about 10% of the full data set).

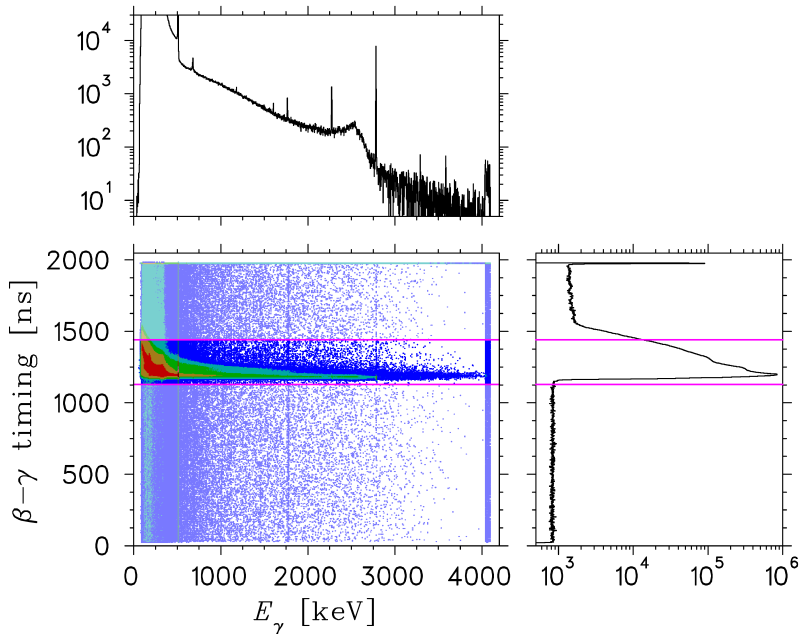

FIG. 4. Density plot of $t_\beta - t_\gamma$ versus E_γ with projections. Good β-γ events are correlated in time, with the acceptance window defined by the two horizontal lines in the 2D plot.

B. Estimation of randoms

As mentioned earlier, every event in the β-γ energy spectra also has the coincidence timing $t_\gamma - t_\beta$ saved eventy-by-event. This allows us to separate genuine coincidence events from the purely random ones where a β particle just happens make it to the scintillator when a random γ ray is detected by the HPGe. Inevitably there are many such γ rays as demonstrated in Fig. 4, however almost all genuine events lie in a small time difference interval. The acceptance window defined by the timing cuts indicated in the figure removes the majority of the random events from the spectral analysis. However, the randoms are also within this window as well, so we must account for the signal-to-noise of our accepted events. This is estimated by looking at the regions where all events are random (left and right side of the peak in the time-difference projection plot on the right panel) and normalizing their combined spectra into the region that was considered to be mostly genuine. This allows the removal of the randoms in the γ spectrum and provides the most optimal signal with minimal background.

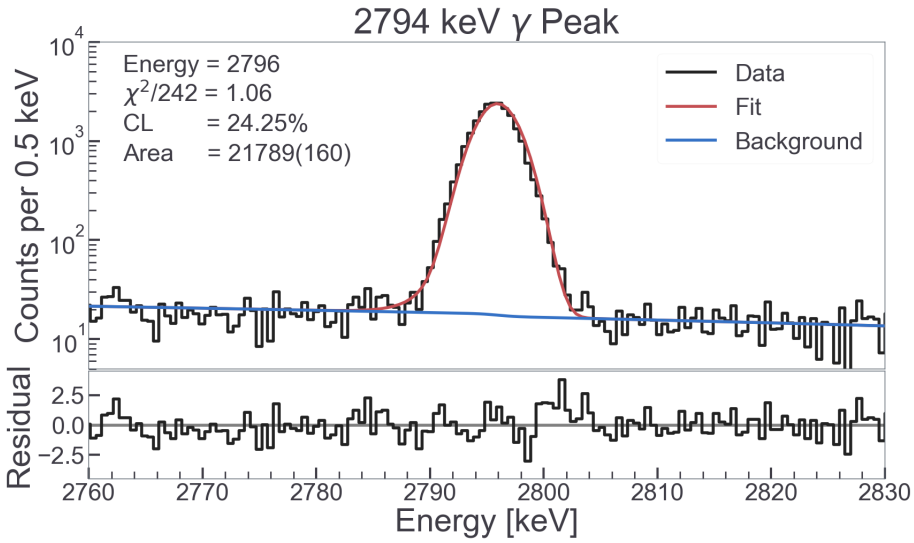

FIG. 5. A fit to the dominant 2796 keV γ-ray. This branch represents the largest fraction of the decays and is therefore the largest contributor to the total uncertainty.

IV. SPECTRAL ANALYSIS

A. γ spectrum and fitting of the peaks

The known γ rays of energies 1184, 1611, 2796 and 3602 keV [3] were identified and fitted with a Gaussian for an energy calibration and characterization of the FWHM of the detector's response. The dominant 2796-keV peak contained enough statistics for a more complete picture, thus fitted with a dominant Gaussian and a small exponential tail to account for incomplete charge collection. Additionally an error function connects the two sides of the linear background. This fit is shown in Fig. 5. Such fits of photopeaks provide the areas that represents the population of a given decay channel while accounting for the proper statistics.

B. β ΔE spectrum, simulation and defining of the threshold

The β spectrum is simulated via Monte Carlo program with 10 keV energy resolution [7]. Simulation spectra is fitted to the experimental spectra with the energy calibration and Gaussian noise convolution. Using the energy calibration from the fitted spectrum, the β detector threshold energy is identified (see 10keV on Fig. 8b), and branch efficiencies as well as overall

average β efficiency is obtained.

V. EXPERIMENTAL CORRECTIONS

A. Rate-dependent corrections

The corrections described here depend on the rate of the events in a given cycle and are therefore corrected cycle-by-cycle. We begin with the expression for the overall correction which we derived [7], and then discuss how each correction was evaluated. If $R_{\text{obs}}(t)$ is the observed rate of β-γ coincidences, then the true rate, $R(t)$, is:

$$R(t) = R_{\text{obs}}(t) \left[\frac{\exp\left(\frac{\eta_\beta \tau_{\text{prompt}}}{1-\eta_\beta\tau_\beta}\right)(1-\eta_{\beta\text{-bkgd}})(1-\eta_\beta\tau_\beta)}{(1-\eta_{\text{coin}}\tau_{\text{busy}})(1-\eta_\gamma\tau_{\text{pile-up}})(1-\eta_\gamma\tau_\gamma)} \right]. \quad (1)$$

Here η_i is the rate of $i = \beta$'s (η_β), γ's (η_γ), β-γ coincidences (η_{coin}), and β background events ($\eta_{\beta\text{-bkgd}}$). A correction is applied for each effect which cause a loss of events, each with a characteristic dead-time: τ_β for the dead-time in the β-singles channel; similarly the dead-time in the γ-singles channel, τ_γ; $\tau_{\text{pile-up}}$ for pile-up events, τ_{prompt} for time peak in time spectrum; and τ_{busy} for the time the acquisition is busy.

Dead-time: Dead-time refers to the blocked time of the detector, system electronics or data acquisition where after the first registered event a second one cannot be detected for a given duration. The probability of losing an event this way can be estimated via the rate of the corresponding dead time, $\eta_i\tau_i$. Thus the factor $\frac{1}{1-\eta_i\tau_i}$ corrects for these losses.

Pile-up: Pile-up is defined as γ-γ coincidence in the HPGe that happens during the charge collection. This type of coincidence results in the total signal registering as the sum of both individual E_{γ_i}'s. The recorded energy, therefore, will remove events from the photo-peak. As with the dead-time, pile-up is corrected by the factor $\frac{1}{1-\eta_\gamma\tau_{\text{pile-up}}}$.

Pre-emption: As described under estimation of randoms, random coincidences were removed from the spectra. However there exists a non-zero probability that a genuine coincidences can be pre-empted by a random β. Similar to pile-up shifting the energy of a real event, pre-emption shifts the coincidence timing, removing an otherwise good event outside of our timing acceptance window. These events that were preemtively removed are corrected based on a probabilistic estimate by a factor $\exp\left(\frac{\eta_\beta\tau_{\text{prompt}}}{1-\eta_\beta\tau_\beta}\right)$. Figure 6 shows the break-up of the

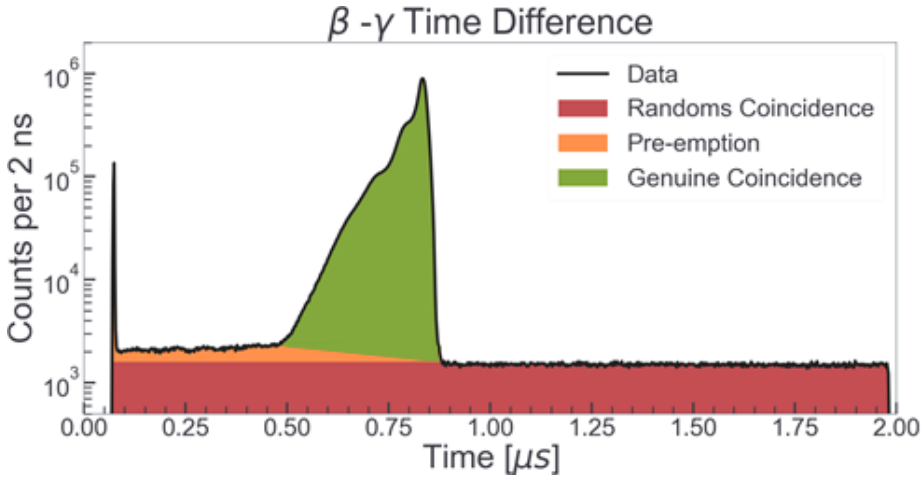

FIG. 6. Coincidence types and time spectrum [7].

β-γ timing spectrum according to genuine coincidences, random coincidences and pre-emptive events.

B. Rate-independent corrections

These corrections do not depend on the rate of events in a given cycle and are therefore corrected collectively.

Annihilation and Bremsstrahlung summing: There is a chance that electron-position annihilation radiation can coincide with the most prominent photo-peak γ rays. This is demonstrated in Fig. 7b where events that would have belong to the 2796-keV peak are shifted by 511 keV, the energy of one of the photons emitted when the e^+-e^- annihilate at rest. These are genuine events that are lost from the branch and must be corrected for. In order to accomplish this correction, one must acquire the correct total-to-peak value of 511 keV photons in a given HPGe detector. The total-to-peak values of all the photo-peaks that come from β decaying isotopes are well known from the efficiency calibration simulations. This is not the case for annihilation γ's due to their source location being not localized; the positrons may travel great distances before encountering an electron and annihilating, and furthermore it may annihilate in-flight. All the photo-peaks summed with their corresponding total-to-peak value are then subtracted from the grand total of the γ spectrum. The difference represents all annihilation γ's (summed and not summed) and bremsstrahlung radiation summing with photo-peaks. The

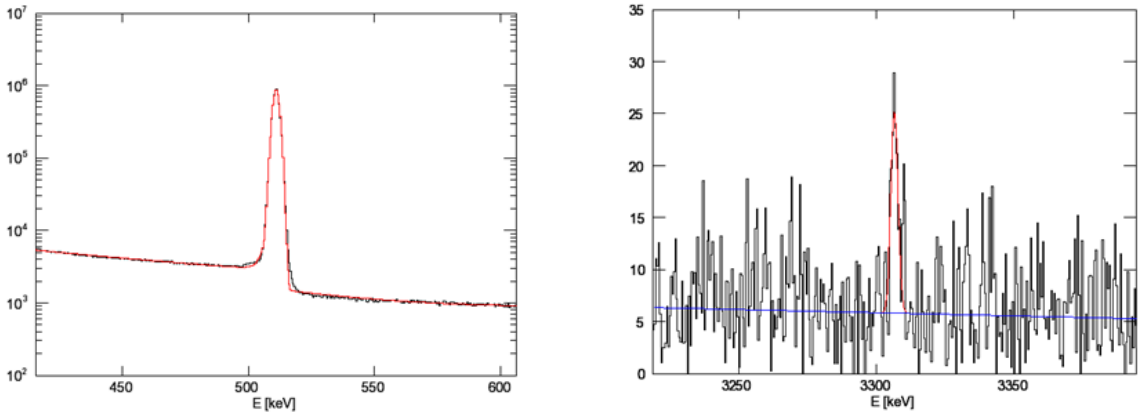

(a) 511-keV peak.

(b) (511+2796)-keV peak.

FIG. 7. γ spectra focused on the annihilation radiation.

actual 511-keV peak area (see Fig. 7a) and the number of summing events gives the 511 effective total-to-peak value with bremsstrahlung radiation effectively accounted in it. This value multiplied to the $2796 + 511 = 3307$-keV peak gives the lost events due to summing effects in the HPGe.

β-singles losses: Focusing on the 0–100 keV range of the β-singles spectrum shown in Fig. 8a, it is seen that in this region there are additional β's from the ridge around 10-keV threshold location. This is due to noise sneaking in through intentionally low set threshold. These events are not genuine events and their contribution must be removed. The linear region where the noise effect is minimal is refitted to properly estimate the β spectra at low energies (green). The number of events above this estimation line are effectively removed from total β count as seen in Fig. 8b.

VI. SUMMING OF THE BRANCHES

γ decay internal conversion competition: Processes that compete with γ decay have to be accounted for losses since we deduce the β branches based on the number of γ-rays emitted from a given excited state in the daughter nucleus. Internal conversion is such a process: an excited nucleus may de-excite by interacting electromagnetically with an orbital electron (which is then ejected from the atom) instead of decaying by γ emission. Thus though the β decay

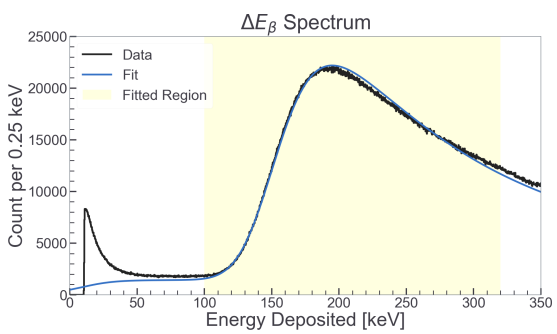

(a) Experimental and simulated β ΔE spectrum.

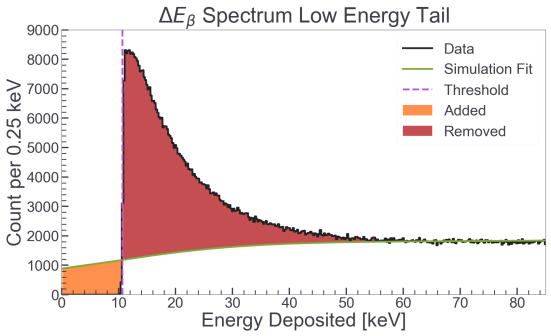

(b) Zoom in of the low-energy portion of the β ΔE spectrum depicting the corrections made to estimate the true number of β events.

FIG. 8. The ΔE spectrum of the thin plastic scintillator used to estimate the number of β singles.

populated the state, there is no γ ray; not including this competetive process would make us underestimate the β branch.

β decay electron capture competition: Competition to β decay must also corrected for. In particular, electron capture is the process by which one of the inner-shell electrons combines with proton to create a neutron and a neutrino. If not accounted for, our deduced branches would be slight underpopulated than what they actually are.

Subtracting the secondary branches: Once the probabilities of the observed branches are found they are added together along with other branches from Ref. [3] that were undetectable to use due to the more limited statistics of the present experiment. This was by design to minimize the summing and pile-up corrections and allow for a very precise measurement of the 2796-keV γ intensity. Our observed branches are added to the others observed in Ref. [3] to get the sum of the β branches to excited states. The branch to the ground state is simply one minus this sum.

VII. RESULTS

Systematic uncertainties that were quantitatively known (the first block of Table I) was propagated as usual. For the remaining, quantitative values were obtained via rigorous process of isolating systematics from every relevant part of the analysis steps to account for any possible bias introduced (second block in Table I). This process involved making objective variations in

TABLE I. Systematic and statistical uncertainties in the branching ratios for the transitions observed. Blank entries indicate an uncertainty below 0.001% and are therefore negligible.

Source	Uncertainty, σ_{BR} [%]			
	$E_\gamma = 1184$ keV	1611 keV	2796 keV	3601 keV
γ efficiencies	–	–	0.011	–
Internal conversion	–	–	–	–
Peak-to-total	–	–	–	–
$t_\beta - t_\gamma$ cuts	0.001	0.001	0.006	0.001
Pre-emption correction	–	–	0.005	–
β/HI cuts	0.001	–	0.004	–
Fitting range	–	–	–	–
Total systematics	0.001	0.001	0.015	0.001
Statistical	0.003	0.003	0.017	0.002
Total uncertainty	0.004	0.003	0.022	0.003

a given systematic procedure and analyzing the response in the final result. The final result for the branching ratio is

$$\mathrm{BR} = 97.81(2)\%, \tag{2}$$

in agreement with the accepted value $\mathrm{BR} = 97.99(14)\%$ [8] but $7\times$ more precise.

Including the statistical rate function $f_V = 3623.9(7)$ from Ref. [8] and $t_{1/2} = 1.23651(94)$ s half-life from Ref. [2], we find

$$ft = 4585(4)\ \mathrm{s}, \tag{3}$$

which is nearly $2\times$ more precise than the previous value of $4576(8)$ calculated using $\mathrm{BR} = 97.99(14)\%$ [8]. Applying, $\delta_R^{'}$ nuclear dependent radiative corrections, δ_{NS}^V nuclear structure corrections and δ_C^V isospin symmetry breaking corrections as described in Ref. [8, 9] we calculate the corrected comparative half-life to be

$$\mathcal{F}t = 4614(5)\ \mathrm{s}. \tag{4}$$

Furthermore using the newest theoretical calculations of $\frac{f_A}{f_V}$ the ratio of phase space integrals of vector vs. axial-vector terms Ref. [10] and experimental measurement of the ρ the Gamow-Teller to Fermi mixing ratio Ref. [1], we find

$$\mathcal{F}t_0 = 6138(32)\ \mathrm{s}. \tag{5}$$

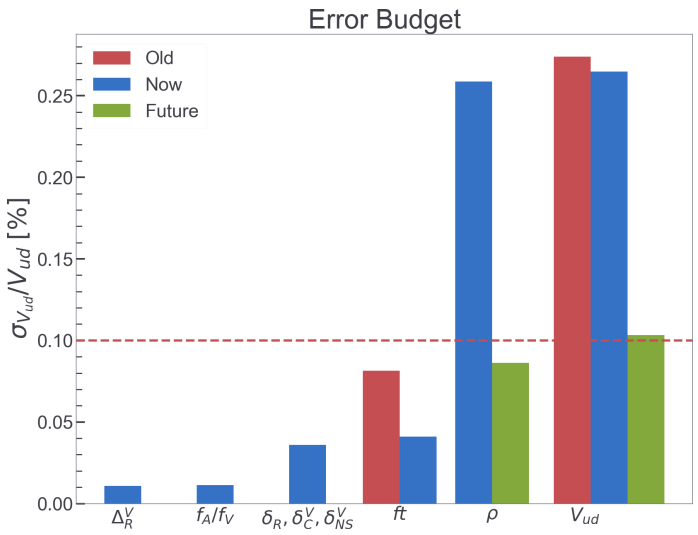

FIG. 9. Final error budget showing; old, current and expected future states of precision.

With the acquired $\mathcal{F}t_0$ value and the application of the universal radiative correction $\Delta_R^V = 0.02467(22)$ of Ref. [11], we finally present our calculation of $|V_{ud}|$:

$$|V_{ud}| = 0.9742(25)_{\rho}(4)_{\text{th}}(4)_{t_{1/2}}(1)_{\text{BR}}. \tag{6}$$

The overall uncertainty in V_{ud} derived from ^{37}K has not signficantly improved due to the difficulty in measuring ρ precisely. The goal of the TRINAT collaboration is to improve the precision of ρ by measuring the β asymmetry parameter, A_β, to $\lesssim 0.1\%$; even when this goal is realized, the ft value will still not contribute to the overall uncertainty, as shown in Fig. 9.

VIII. CONCLUSIONS

Using the fast-tape transport system in conjunction with the world's most precisely calibrated HPGe of its kind, we improved the uncertainty in the branching ratio by a factor of 5. This has doubled the precision of the ft value which is being used to test the standard model. With our contribution, uncertainties in the ft value will remain negligible even after precision of ρ is measured to $\lesssim 0.1\%$.

[1] B. Fenker *et al.*, Phys. Rev. Lett. **120**, 062502 (2018).

[2] P. Shidling *et al.*, Phys. Rev. C **90**, 032501(R) (2014).
[3] E. Hagberg *et al.*, Phys. Rev. C **56**, 135 (1997).
[4] R. Helmer *et al.*, Nucl. Instrum. Methods Phys. Res. A **511**, 360 (2003).
[5] R. Helmer *et al.*, Appl. Radiat. Isot. **60**, 173 (2004).
[6] M. Bencomo, Ph.D. thesis, Texas A& M University (2019).
[7] V. Iacob (2020), private communication.
[8] N. Severijns *et al.*, Phys. Rev. C **78**, 055501 (2008).
[9] O. Naviliat-Cunic and N. Severijns, Phys. Rev. Lett. **102**, 142302 (2009).
[10] L. Hayen and N. Severijns (2019), arXiv:1906.09870.
[11] C.-Y. Seng *et al.*, Phys. Rev. Lett. **121**, 241804 (2018).